Short Papers

Energy and Power Relations for an Electron Beam in a Cylindrical Waveguide

S. R. SESHADRI, SENIOR MEMBER, IEEE

Abstract—**The characteristics of the energy per unit length and power flow are analyzed for the transverse magnetic mode supported by an electron beam drifting with a relativistic velocity parallel to the axis of a cylindrical waveguide. The parts of the dispersion curve corresponding to the positive and the negative energy waves are identified.**

I. Introduction

The development of relativistic electron beams has revived interest in the free electron sources of microwaves, particularly at millimeter wavelengths [1]–[4]. It is important to understand the characteristics of the average energy and power flux densities of the electron beam. These characteristics of a transversely unbounded electron beam are customarily used to interpret the results obtained for an electron beam in a drift tube. In this short paper we deduce the characteristics of the energy per unit length and power flow in a cylindrical electron beam.

II. Expressions for Energy and Power

A perfectly conducting cylindrical waveguide of radius a has its axis coincide with the z-axis of a cylindrical coordinate system r, ϕ, and z. Filling the waveguide uniformly and drifting with a velocity $\hat{z}v_d$ is a fully neutralized electron beam characterized by the angular plasma frequency ω_p. The electron beam is guided by an axial magnetostatic field which is sufficiently strong to suppress the transverse motions of the electrons. The perturbed quantities vary as $\exp[-i(\omega t - kz)]$. Then, the electron beam behaves like a dielectric [5] characterized by the permittivity tensor $\epsilon = \epsilon_0(\hat{r}\hat{r} + \hat{\phi}\hat{\phi} + \hat{z}\hat{z}\epsilon_{zz})$ where

$$\epsilon_{zz} = 1 - \omega_p^2\alpha^2/(\omega - kv_d)^2. \tag{1}$$

The relativistic factor α is given by $\alpha = [1-(v_d/c)^2]^{1/2}$ where c is the velocity of electromagnetic waves in free space. Sometimes $\gamma = 1/\alpha$ is used as the relativistic factor [2], [6]. In (1) $\omega_p^2 = Ne^2\alpha/m_0\epsilon_0$ where N is the number density of the electron beam in the laboratory frame, $-e$ is the electronic charge, m_0/α is the mass of an electron in the laboratory frame and ϵ_0 is the free-space permittivity. The plasma frequency defined in this manner has the advantage of being a relativistic invariant. The fields are assumed to be azimuthally symmetric ($\partial/\partial\phi = 0$). We shall consider only the TM-modes having the nonvanishing field components H_ϕ, E_r, and E_z since they include the space charge waves. Together with (1), from Maxwell's equations, we find that [7]–[9]

$$H_\phi = \frac{i\omega\epsilon_0 c^2}{(\omega^2 - k^2c^2)}\frac{\partial E_z}{\partial r} \tag{2a}$$

$$E_r = \frac{ikc^2}{(\omega^2 - k^2c^2)}\frac{\partial E_z}{\partial r} \tag{2b}$$

and

$$\left[\frac{\partial^2}{\partial r^2} + \frac{1}{r}\frac{\partial}{\partial r} + p^2\right]E_z = 0 \tag{3}$$

where

$$p^2 = (\omega^2/c^2 - k^2)\epsilon_{zz}. \tag{4}$$

The solution of (3), subject to the requirement that E_z is finite for $r = 0$ and the boundary condition that $E_z = 0$ for $r = a$, yields

$$E_z = E_0 J_0(p_{0n}r/a) \tag{5}$$

where E_0 is a constant and p_{mn} is the nth zero of Bessel function of order m. Also, with the help of (1) and (4), ω and k can be shown to be governed by the dispersion relation

$$F(\omega, k) = \frac{\omega_p^2\alpha^2}{(\omega - kv_d)^2} + \frac{(p_{0n}c/a)^2}{(\omega^2 - k^2c^2)} = 1. \tag{6}$$

Substituting (5) in (2a, b) gives

$$H_\phi = -\frac{i\omega\epsilon_0 c^2}{(\omega^2 - k^2c^2)}\left(\frac{p_{0n}}{a}\right)E_0 J_1(p_{0n}r/a) \tag{7a}$$

$$E_r = -\frac{ikc^2}{(\omega^2 - k^2c^2)}\left(\frac{p_{0n}}{a}\right)E_0 J_1(p_{0n}r/a). \tag{7b}$$

When the energy density in the magnetic field $w_H = 1/4\,\mu_0|H_\phi|^2$ is integrated throughout the cross section of the waveguide, we obtain that

$$W_H = \frac{\pi\omega^2c^2\epsilon_0|E_0|^2}{4(\omega^2 - k^2c^2)^2}p_{0n}^2 J_1^2(p_{0n}). \tag{8}$$

When the energy density in the electric field

$$w_E = \frac{1}{4}\boldsymbol{E}^* \cdot \frac{\partial}{\partial\omega}(\omega\boldsymbol{\epsilon}) \cdot \boldsymbol{E} = \frac{1}{4}\epsilon_0|E_r|^2 + \frac{1}{4}\epsilon_0\frac{\partial(\omega\epsilon_{zz})}{\partial\omega}|E_z|^2$$

is integrated throughout the cross section of the waveguide, it is found that

$$W_E = \frac{\pi k^2c^4\epsilon_0|E_0|^2}{4(\omega^2 - k^2c^2)^2}p_{0n}^2 J_1^2(p_{0n}) + \frac{\pi\epsilon_0}{4}\left(\frac{\partial\omega\epsilon_{zz}}{\partial\omega}\right)|E_0|^2 a^2 J_1^2(p_{0n}). \tag{9}$$

Adding (8) and (9), and using (1) and (6), we express the energy for unit length of the electron beam inside the cylindrical waveguide as

$$W = W_H + W_E = C\omega\left[\frac{(p_{0n}c/a)^2\omega}{(\omega^2 - k^2c^2)^2} + \frac{\omega_p^2\alpha^2}{(\omega - kv_d)^3}\right] \tag{10a}$$

$$= -C\frac{\omega}{2}\frac{\partial F}{\partial\omega} \tag{10b}$$

where

$$C = \pi\epsilon_0 a^2|E_0|^2 J_1^2(p_{0n})/2. \tag{11}$$

Note that C is a positive real constant for all values of ω and k.

When the Poynting vector $\boldsymbol{S}_p = 1/2\ \mathrm{Re}(\boldsymbol{E} \times \boldsymbol{H}^*)$ is integrated

Manuscript received October 10, 1981; revised November 23, 1981.

The author is with the Department of Electrical and Computer Engineering, University of Wisconsin, Madison, WI 53706.

0018-9480/82/0500-0813$00.75 ©1982 IEEE

throughout the cross section of the waveguide, we find that

$$S_p = \hat{z}\frac{\pi k\omega c^4\epsilon_0|E_0|^2}{2(\omega^2-k^2c^2)^2}p_{0n}^2J_1^2(p_{0n}). \tag{12}$$

Similarly, when the kinetic power flux density [10] $S_k = -1/4\ E^*\cdot(\partial\omega\epsilon/\partial k)\cdot E$ is integrated throughout the cross section of the waveguide, on noting that ϵ is a function of only $k=\hat{z}k$, we can show that

$$S_k = \hat{z}\frac{\pi\omega\omega_p^2\alpha^2v_d\epsilon_0|E_0|^2}{2(\omega-kv_d)^3}a^2J_1^2(p_{0n}). \tag{13}$$

Adding (12) and (13), the total power flow through the waveguide is obtained as

$$S = S_p + S_k = \hat{z}S = \hat{z}C\omega\left[\frac{kc^2(p_{0n}c/a)^2}{(\omega^2-k^2c^2)^2}+\frac{\omega_p^2\alpha^2v_d}{(\omega-kv_d)^3}\right] \tag{14a}$$

$$= \hat{z}C\frac{\omega}{2}\frac{\partial F}{\partial k}. \tag{14b}$$

The group velocity can be deduced from the kinematic considerations using (6) with the following result:

$$v_g = \frac{d\omega}{dk} = \hat{z}\frac{d\omega}{dk} = -\hat{z}\frac{\partial F}{\partial k}\Big/\frac{\partial F}{\partial\omega}. \tag{15}$$

The group velocity can also be evaluated from the dynamic considerations using (10b) and (14b) as $v_g = S/W$ which, as it should be, is equal to that deduced in (15).

It is seen that $F(\omega,k)$, W, and S are invariant under the transformation $\omega\to-\omega$ and $k\to-k$. This symmetry enables us to treat these quantities for only positive values of ω. An analysis of (6) shows that there is a field wave (FW) which exists for ω above a cutoff value which is slightly below $[\omega_p^2\alpha^2 + (p_{0n}c/a)^2]^{1/2}$. At the minimum value of ω of propagation of the field wave, k is slightly negative. For $k>0$, for the FW, $\omega > kv_d$. There are two space charge waves (FSW, SSW). For relativistic velocities, $k>0$ for the two space charge waves (see Fig. 1(a)). For the fast space charge wave (FSW), ω is slightly greater than kv_d and for the slow space charge wave (SSW) ω is slightly less than kv_d. For nonrelativistic velocities, that is for v_d/c sufficiently less than unity, the space charge wave SSW has another branch (SSWN) for which $k<0$ (see Fig. 1(b)).

For $k<0$, (10a) shows that $W>0$. For $k>0$, if $\omega>kv_d$, again (10a) shows that $W>0$. Therefore, it follows that W for the wave FW, the space charge wave FSW, and the branch SSWN of the space charge wave SSW are all positive. These results can be confirmed and the sign of W of the wave SSW can also be obtained by examining the plot of F as a function of ω for $k>0$ as shown in Fig. 2(a) for relativistic velocities and in Fig. 2(b) for sufficiently small nonrelativistic velocities. For $|\omega|>kc$, it is seen from (6) that $F>0$. For $|\omega|\to\infty$, $F\to0$. At $\omega=\pm kc$, F becomes infinite and changes sign. $F\to+\infty$ as $\omega\to kv_d$ from either side. F can be shown to have two real zeros for $|\omega|<kc$. These zeros occur in the ranges $kv_d<\omega<kc$ and $-kc<\omega<kv_d$. For the latter zero, $\omega>0$ for relativistic velocities and $\omega<0$ for sufficiently small nonrelativistic velocities. Also, (6) shows that F is a monotonically increasing function of ω for $\omega<kv_d$ and a monotonically decreasing function of ω for $\omega>kv_d$. Only the shape of F as a function of ω for positive values of F is required. The intersection points of the various branches of the curve F with the straight line $F=1$ correspond to the solutions of (6). The various branches of the dispersion curves shown in Fig. 1 are related to the various branches of the curve F, as indicated in Fig. 2. Since $\partial F/\partial\omega<0$ for the FW and the FSW branches, it follows

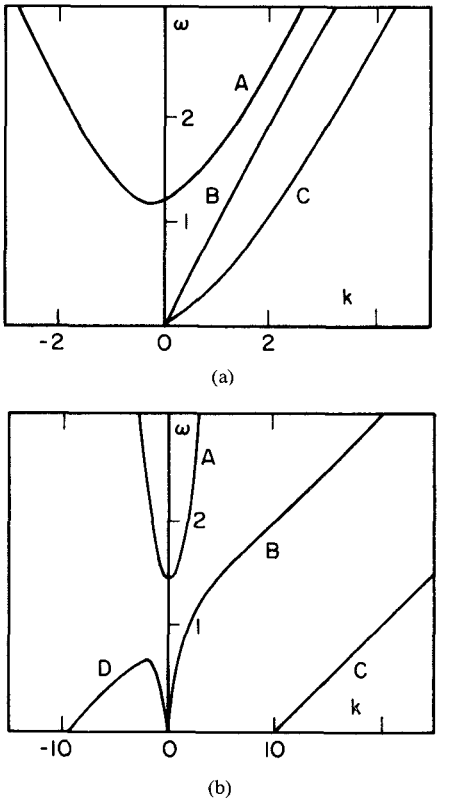

Fig. 1. Dispersion curves for (a) relativistic velocities and (b) sufficiently small nonrelativistic velocities A: field wave (FW); B: fast space charge wave (FSW); C: slow space charge wave (SSW); D: the branch (SSWN) of the slow space charge wave.

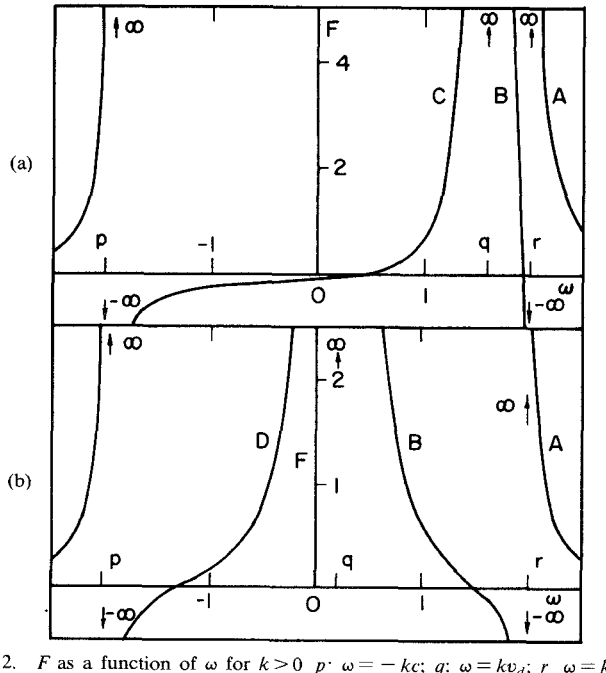

Fig. 2. F as a function of ω for $k>0$ p: $\omega=-kc$; q: $\omega=kv_d$; r $\omega=kc$. Other symbols are the same as in Fig. 1

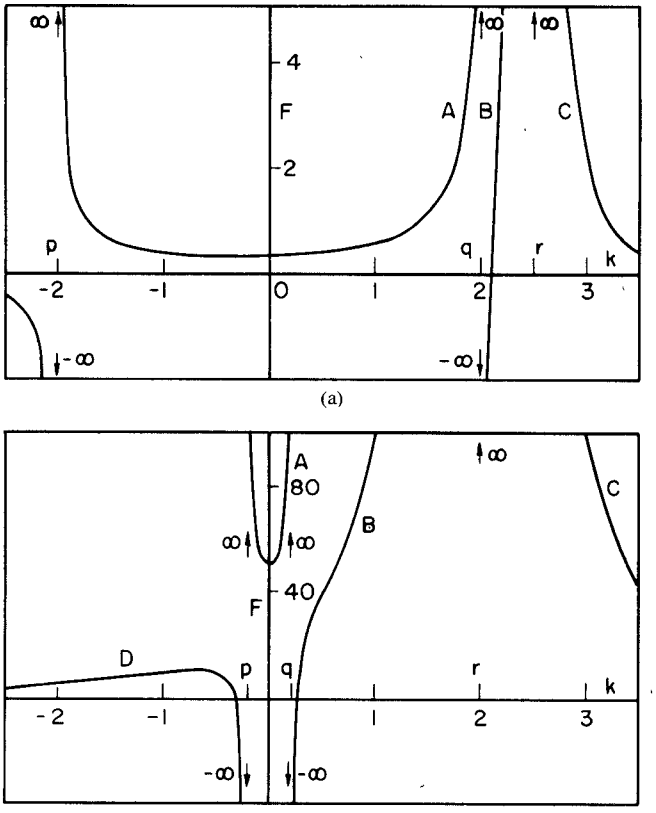

Fig. 3. F as a function of k for $\omega > 0$. p: $k = -\omega/c$; q: $k = \omega/c$; r: $k = \omega/v_d$. Other symbols are the same as in Fig. 1.

from (10b) that $W > 0$. For the SSW branch, since $\partial F/\partial\omega$ and ω are positive, (10b) shows that $W < 0$. Using the symmetry under the transformation $\omega \to -\omega$ and $k \to -k$ yields that the part of the SSW branch having $\omega < 0$ corresponds to the SSWN branch. For this branch, since $\partial F/\partial\omega > 0$ and $\omega < 0$, from (10b) we see that $W > 0$. Thus, the energy per unit length of the electron beam is positive for all branches of the dispersion curve except the SSW branch ($0 < \omega < kv_d$) for which $W < 0$.

III. Sign of Energy and Power

For $k > 0$ and $\omega > kv_d$, (14a) shows that $S > 0$, that is for the part with $k > 0$ of the wave FW and for the wave FSW, the total power flow in the direction of the beam is positive. The sign of S for the remaining branches of the dispersion curve can be ascertained by examining the plot of F as a function of k for $\omega > 0$ as shown in Fig. 3(a) for relativistic velocities and in Fig. 3(b) for sufficiently small nonrelativistic velocities. For $|k| < \omega/c$, it is seen from (6) that $F > 0$. At $k = \pm\omega/c$, F becomes infinite and changes sign. Therefore, as k is increased from $-\omega/c$ to $+\omega/c$, F decreases from $+\infty$, reaches a positive minimum value, and then increases to $+\infty$. $F \to +\infty$ as $k \to \omega/v_d$ from either side. Hence, it follows from (6) that as k is increased from ω/c to ω/v_d, F increases monotonically from $-\infty$, goes through zero to $+\infty$. F is zero for two finite real values of k. As mentioned previously, one of the zeros occurs in the range $\omega/c < k < \omega/v_d$. For relativistic velocities corresponding to $p_{0n}/a > \omega_p\alpha/v_d$, the second zero occurs in the range $\omega/v_d < k < \infty$. For this case, $F < 0$ for $|k| \to \infty$. Therefore, as k is increased from ω/v_d to ∞, F decreases from $+\infty$ monotonically to zero, goes negative, reaches a negative minimum value, and then monotonically increases to negative zero (not fully shown in Fig. 3(a)). As k decreases from $-\omega/c$ to $-\infty$, F increases monotonically from $-\infty$ to negative zero. For sufficiently small nonrelativistic velocities corresponding to $p_{0n}/a < \omega_p\alpha/v_d$, the second zero of F occurs in the range $-\infty < k < -\omega/c$. For this case, $F > 0$ for $|k| \to \infty$. Therefore, as k is increased from ω/v_d to ∞, F decreases monotonically from $+\infty$ to positive zero (see Fig. 3(b)). As k decreases from $-\omega/c$ to $-\infty$, F increases from $-\infty$ monotonically to zero, goes positive, reaches a positive maximum value, and then monotonically decreases to positive zero. As before, only the shape of F as a function of k for positive values of F is required. The intersection points of the various branches of the curve F with the straight line $F = 1$ corresponds to the solutions of (6). The various branches of the dispersion curve shown in Fig. 1 are related to the various branches of the curve F, as indicated in Fig. 3. For $k > k_{\min}$ (which is negative) for the wave FW, for the space charge wave FSW and for $k < k_{\max}$ (which is negative) for the branch SSWN of the space charge wave SSW, since $\partial F/\partial k > 0$, (14b) shows that $S > 0$. For $k < k_{\min}$ of the wave FW, for the wave SSW and for $k > k_{\max}$ of the wave SSWN, since $\partial F/\partial k < 0$, it follows from (14b) that $S < 0$. In other words, for the space charge wave SSW, $S < 0$. For all other branches of the dispersion curve, the sign of S is the same as the sign of the slope of the dispersion curves (shown in Fig. 1) with respect to k.

IV. Conclusion

In conclusion, we have deduced the energy per unit length and power flow in an electron beam contained by a cylindrical waveguide.

REFERENCES

[1] J. E. Walsh, T. C. Marshall, M. R. Mross, and S. P. Schlesinger, "Relativistic electron-beam-generated coherent submillimeter wavelength Cerenkov radiation," *IEEE Trans. Microwave Theory Tech.*, vol. MTT-25, pp. 561–563, June 1977.

[2] J. E. Walsh, "Cerenkov and Cerenkov-Raman radiation sources," in *Free-Electron Generators of Coherent Radiation*, S. F. Jacobs, H. S. Pilloff, M. Sargent III, M. O. Scully, and R. Spitzer, Eds. Reading, MA: Addison-Wesley, 1980, pp. 255–300.

[3] T. C. Marshall, S. P. Schlesinger, and D. B. McDermott, "The free-electron laser: A high-power submillimeter radiation source," in *Advances in Electronics and Electron Physics*, vol. 53, L. Marton and C. Marton, Eds. New York: Academic Press, 1980, pp. 47–84.

[4] R. S. Symons and H. R. Jory, "Cyclotron resonance devices," in *Advances in Electronics and Electron Physics*, vol. 55, edited by L. Marton and C. Marton, Eds. New York: Academic Press, 1981, pp. 1–75.

[5] R. E. Collin, *Foundations for Microwave Engineering*. New York: McGraw-Hill, 1966, pp. 439–446.

[6] P. F. Ottinger and J. Guillory, "Beam-plasma interactions in a filled waveguide immersed in applied axial magnetic field," *Phys. Fluids*, vol. 22, pp. 466–475, Mar. 1979.

[7] A. W. Trivelpiece and R. W. Gould, "Space charge waves in cylindrical plasma columns," *J. Appl. Phys.*, vol. 30, pp. 1784–1793, 1959.

[8] R. W. Gould and A. W. Trivelpiece, "A new mode of wave propagation on electron beams," in *Proc. Symp. Electronic Waveguides* edited by J. Fox, Ed. New York: Polytechnic Press, 1958, pp. 215–228.

[9] A. W. Trivelpiece, *Slow-Wave Propagation in Plasma Waveguides*. San Francisco CA: San Francisco Press, 1967, pp. 8–19.

[10] W. P. Allis, S. J. Buchsbaum, and A. Bers, *Waves in Anisotropic Plasmas*. Cambridge, MA: M.I.T. Press, 1963, pp. 121–126.

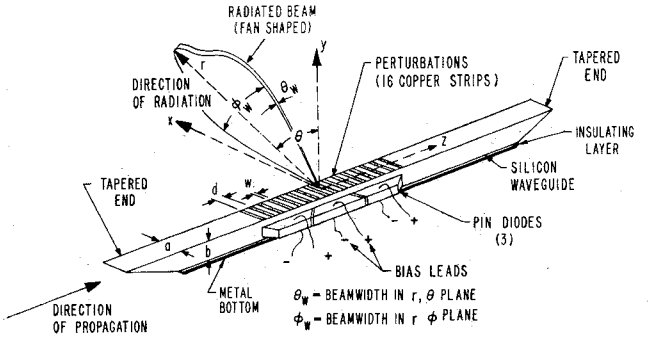

Fig. 1. Line scanning antenna, configuration.

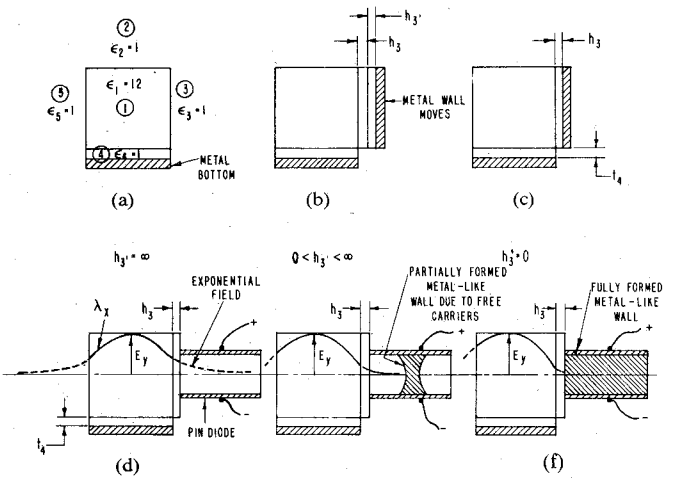

Fig. 2. Silicon waveguide, cross section, and *E*-field distribution. (a) Diodes unbiased (ideal), (b) diodes partially biased (ideal), (c) diodes fully biased (ideal), (d) field distribution diodes unbiased, (e) *E*-field distribution diodes small bias, (f) *E*-field distribution diodes fully biased.

Single-Frequency Electronic-Modulated Analog Line Scanning Using a Dielectric Antenna

R. E. HORN, SENIOR MEMBER, IEEE, H. JACOBS, FELLOW, IEEE, K. L. KLOHN, MEMBER, IEEE, AND E. FREIBERGS, MEMBER, IEEE

***Abstract*—A line scanning antenna is described whereby means of periodic perturbations and conductivity changes in p-i-n diode modulators, analog angular shifts of 5° can be obtained. The system is electronically modulated with relatively small power requirements.**

I. INTRODUCTION

In a recent report [1], an electronic modulated beam-steerable silicon waveguide array antenna was described. The construction of this device is shown in Fig. 1. It consisted of a silicon dielectric waveguide (runner), the ends of which were inserted into a metal waveguide and operated in the region of 60 to 70 GHz. The overall circuit arrangement was also described in the above referenced report. The basic concept for the operation of this device is as follows. As the energy propagates down the dielectric runner, an evanescent portion of the wave is in the air space surrounding the dielectric (Fig. 2) both in the vertical and horizontal directions. The perturbations on the top surface (copper strips) transform propagated energy to radiation. At any given frequency, the angle of radiation is a function of the guide wavelength λ_z and the perturbation spacing d. In this arrangement, d is fixed but the guide wavelength can be modified by the p-i-n diode modulators attached to the runner side wall. If the diodes are unbiased the wave will continue propagating down the runner with a guide wavelength λ_z. When the diodes are biased in the forward direction, they become conductive and act as if a conductive wall were placed on the runner sidewall (Fig. 2). This results in a new guide wavelength λ_z'. The result of the change in wavelength is that the radiation angle θ is changed, thus giving a line scan. The problem here is that the line scan is digital. There is a loss which occurs with an increase in the current in the modulating p-i-n diodes from 0 level to higher bias currents. This was shown in [1], where with zero bias an expected radiation pattern is obtained. With 300 mA (100 mA per diode) the pattern is shifted, $\Delta\theta = 9.5°$, but at intermediate currents, the radiation pattern deteriorated (i.e., attenuated and broadened). This behavior can be explained by realizing absorption of energy by the p-i-n diode modulators occurs when the diode current is low, since the conductivity of the intrinsic (I) region is intermediate between an insulator and a metallike conductor. In the intermediate conductivity state, the energy is not only being absorbed but is refracting into the lossy intrinsic medium. The fields in the runner and p-i-n modulator are envisaged as shown

Manuscript received September 4, 1981; revised November 23, 1981.

The authors are with the U.S. Army Electronics Technology and Devices Laboratory, Fort Monmouth, NJ 07703.